Bull. Mater. Sci., Vol. 25, No. 6, November 2002, pp. 521–526. © Indian Academy of Sciences.

Thermal sensor properties of PANI(EB)–CSA_X ($X = 0{\cdot}4 \pm 0{\cdot}1$ mol) polymer thin films

T PRAKASH*, S A K NARAYAN DASS† and K PREM NAZEER†

Department of Nuclear Physics, Madras University, Chennai 600 025, India
†Department of Physics, Bharathiar University, Coimbatore 641 046, India

Abstract. Films of polyaniline(EB) doped with camphor sulfonic acid (CSA) from *m*-cresol on glass substrates exhibit considerable metallic properties. Such polymer metallic films have thermal sensitivity superior to ceramic metal (Cermet) films, prepared by metallo organic deposition (MOD) technique on silicon substrates. These PANI(EB)–CSA_X (X = 0·5, 0·4, 0·3 mol) polymer films were developed through controlled temperature atmosphere 60 ± 2°C for 60 min, and with the help of temperature dependence of resistivity (r) values, high temperature coefficient of resistance (TCR) i.e. a values, and figure of merit (ra) values of these films, thermal sensitivity were compared from that we observed. Among the three doping ratios the PANI(EB)–$CSA_{0{\cdot}3\ mol}$ film (4·4 μm thick) on glass substrate resistivity (r) values in the range of 838–1699 Ω·μm with high TCR i.e. a = 10,291 ppm/°C and figure of merit (ra) value in range of 8·62–17·48 Ωm/°C seems to be the best. This paper deals with these superior thermal-sensing properties together with optical studies and surface topography by atomic force microscopy (AFM). These polymer films offer design advantages in developing 'thin film polymer thermal sensor'.

Keywords. AFM; thermal sensor; solution casting techniques; temperature coefficient of resistance; polyaniline(EB).

1. Introduction

Resistor films on silicon or other insulating (e.g. glass, fused SiO_2, Al_2O_3) substrates, with high temperature coefficient of resistance (a) and wide resistivity (r) range are in high demand for many types of sensing applications (Chopra and Kaur 1983). This paper describes the thermal sensor properties of electrically conductive PANI(EB)–CSA_X (X = 0·5, 0·4, 0·3 mol) polymer solution cast films on glass substrates. The higher figure of merit (ra) of these films makes them superior to the Pt, Ni and alloy based metal films, which are widely used in film heaters, thermistors, and bolometers. Chopra (1969) and Sundeen and Buchanan (2001) recently reported thermal sensitivity of Ni–ZrO_2 cermet films (~ 1·0 μm thick) deposited on silicon substrates by metallo-organic deposition (MOD) technique. For thermal sensor use a high TCR is desired and defined as

$$\mathrm{TCR} = \frac{[R_{T_2} - R_{T_1}]}{[R_{T_1}(T_2 - T_1)]} \cdot 10^6, \tag{1}$$

where TCR, in other words, a, is expressed in ppm/°C and R_{T_1} and R_{T_2} are sheet resistance values at temperature T_1 and T_2, respectively. The TCR is often described using T_2 = 125°C and T_1 = 25°C and is referred to as hot TCR. A figure of merit for thermal sensors has been defined as the product of resistivity and TCR (i.e. ra) with unit of Ωm/°C. The figure of merit is based on the maximum resistance response to temperature (dR/dT), and is expressed as,

$$\left[\frac{\mathrm{d}R}{\mathrm{d}T}\right] = a\, R_{T_1} = \frac{[r\, a\, l]}{A}, \tag{2}$$

where r is the resistivity at temperature T_1, thus [dR/dT] is directly related to ra, and is modulated by the length to area (l/A) ratio of the resistor. According to the Methiessen's rule, the ra product is generally constant for metal systems (Mott and Jones 1958; Maissel and Glang 1970).

2. Experimental

2.1 *Materials*

Aniline (purchased from Aldrich), *m*-cresol (purchased from Merck), HCl, acetone, NH_4OH, $(NH_4)_2S_2O_8$ and camphor sulfonic acid (CSA) were used in as received condition.

2.2 *Synthesis of polyaniline(EB) powder*

30 ml conc. HCl, 44 ml acetone and 176 ml distilled water were mixed into 250 ml solution. 180 ml of the

*Author for correspondence

solution and 10 ml of aniline were added into a 500 ml flask (covered with ice cubes–salt mixtures to maintain low polymerization temperature) equipped with electromagnetic stirrer. 22·8 g of $(NH_4)_2S_2O_8$ (ammonium per oxy disulphate) was dissolved into the remaining 70 ml of the solution, this mixture was then added into the reactor drop by drop for 1 h. The polymerization temperature 0–5°C was maintained for 5 h to complete the reaction. Then the precipitate obtained was filtered using G2 sintered glass filter. The product was washed successively by distilled water (250 ml) and methanol (150 ml), respectively until the wash solution turned colourless. Then it was re-filtered and washed once again successively by one mol of distilled water, acetone, diethyl ether and 250 ml of NH_4OH, thoroughly to obtain the emeraldine base form of polyaniline, then dried at 60°C for 24 h. Thus, finally obtained powder (Geng *et al* 1998) of insulating polyaniline(EB) polymer and its structure (Pouget *et al* 1991) is shown in figure 1.

2.3 *Synthesis of PANI(EB)–CSA$_X$ polymers*

PANI(EB) complexed with camphor sulfonic acid (CSA) was synthesized (formula weight, 232·30 g) by solid state reaction using the procedure reported by Cao *et al* (1995). We followed the same doping process and prepared three different ratios (X = 0·5, 0·4, 0·3 mol) of doped PANI(EB) polymers. 91 g of PANI(EB) with the corresponding mol amount of CSA was grounded well in a dried mortar for more than 0·5 h. The fine powder thus obtained is the required doped PANI(EB) polymer.

2.4 *Solubility test*

The solubility of PANI(EB) in *m*-cresol has been reported by Tang *et al* (1996). So, we examined the solubility of PANI(EB)–CSA$_X$ (X = 0·5, 0·4, 0·3 mol) polymers with the same solvent *m*-cresol, by adding 0·1 g of PANI(EB)–CSA$_X$ polymers into 5 ml of *m*-cresol solvent then stirred for 4 h. The mixture was filtered with G2 sintered glass filter and the precipitate obtained was washed for several times with the same solvent. PANI(EB)–CSA$_X$ was completely soluble without residual in the filter that was checked by weighing the filter after and before the filtering process with the help of digital micro-balance.

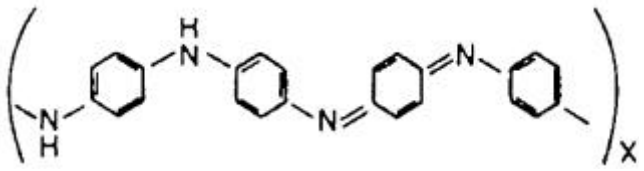

Figure 1. Structure of polyaniline(EB) polymer.

2.5 *Films by solution casting technique*

As indicated, the polymer films were developed using the 'solution casting method'. The required solution was prepared, by adding 5 ml of *m*-cresol with 0·1 g of polymer powder and stirred well for 4 h. The solution was filtered with the help of G2 sintered glass filter and collected in sample bottles and kept at room temperature for 14 h. We used a pipet (5–50 µl capacity, Glasco micro pipetor, made in Finland) to cast the polymer solutions on top of cleaned glass substrates. Using that, we prepared various thicknesses of the films by varying the amount of solution that dropped on the horizontally placed substrates and leaving those substrates for 1 h at 60 ± 2°C in hot atmosphere for the solvent to evaporate. But we will not be able to prepare films with the same thickness in this method, which is the main disadvantage, even if we drop the same amount of the solution on the substrates. Using this procedure, we prepared PANI(EB) and PANI(EB)–CSA$_X$ polymer films having approximately equivalent thicknesses only.

2.6 *Characterization*

First of all, the purity of chemically synthesized PANI(EB) polymer powder was examined by FTIR absorption spectra obtained from KBr pellets and the spectrum was recorded on a 'Bruker FTIR spectrometer' in the region 2000–400 cm^{-1}. Optical absorption spectra were recorded at room temperature by 'Hitachi 330 Model Spectrophotometer' in the wavelength region 200–1200 nm for both PANI(EB) and PANI(EB)–CSA$_X$ polymer films. Then electrical properties for various thicknesses of PANI(EB)–CSA$_X$ (X = 0·5, 0·4, 0·3 mol) polymer films on chemically and ultrasonically cleaned glass substrates were studied by standard four-probe method. Those film thicknesses were measured by mechanical micrometer method using universal length measuring instrument (TRIMOS, Switzerland) with an accuracy of ± 0·32 µ. And finally, atomic force microscopy (AFM) scans for study of surface topography were performed using AFM instrument made by Central Scientific Instruments Organization (CSIO), Chandigarh, in air at room temperature.

3. Results and discussion

3.1 *Analysis of FTIR spectra*

The FTIR spectra for the chemically synthesized polyaniline(EB) powder was obtained from KBr pellets, the spectrum was recorded on a 'Bruker spectrometer' at a resolution of 4 cm^{-1}. Figure 2 shows the FTIR absorbance spectra of PANI(EB) polymer powder. The absorbance spectra have the characteristic peaks of PANI(EB) at

1586·1, 1495·7, 1376·9, 1305·8, 1163·3, 1143·7, 1008·1, 953·7, 829·2, 635·0, 507·0, 414·4 cm^{-1} obtained in between the wavelengths 2000–400 cm^{-1}. It matches with the reported (Tang *et al* 1996) characteristic peaks of PANI(EB) particularly, 1590, 1495, 1305, 1165 and 830 cm^{-1}. Compared with the peak at 1495 cm^{-1} and the relative intensity of the peak at 1590 cm^{-1} with the standard reports (Tang *et al* 1989; Geng *et al* 1998), we are satisfied with the synthesis of polyaniline(EB) powder.

3.2 *Optical characterization*

The UV-visible absorption spectra of PANI(EB) and PANI(EB)–CSA$_X$ (X = 0·5, 0·4, 0·3 mol) polymer films were recorded at room temperature by 'Hitachi 330 Model Spectrophotometer'. Base line was corrected before recording the spectra by using chemically and ultrasonically cleaned two glass substrates having same thickness (1·35 mm) which were placed one in the sample position and other one in the reference position. Since the reference used in the experiment was for the films made by the same thickness glass substrates, the surface reflection was eliminated. Spectra were scanned at the flow rate 100 nm/min. Absorption spectra of PANI(EB) and PANI(EB)–CSA$_X$ (X = 0·5, 0·4, 0·3 mol) polymer films were recorded in the wavelength region 200–1200 nm. Typical absorption spectra for all the polymer films are shown in figure 3. The uncertainties in the absorbance values are within the ± 0·002 nm. Films used to record the spectra are not in same thickness (9·3 μm for PANI(EB), 8·0 μm for PANI(EB)–CSA$_{0·5\ mol}$, 7·7 μm for PANI(EB)–CSA$_{0·4\ mol}$, 4·4 μm for PANI(EB)–CSA$_{0·5\ mol}$), since in the solution casting technique, we are not able to prepare all the films with the same thickness.

The UV-visible absorption spectra of PANI(EB) in *m*-cresol solution cast film gives absorption bands at 423 nm and 675 nm. In this case, the l_{max} (wavelength of an absorption maximum) is 423 nm and this band has been assigned as the p–p^* transition and the band at 675 nm is due to electron band arising due to the shifting of electron from benzenoid ring to quinoid ring. In all the doped polyaniline cases, only the p–p^* transition band alone of PANI(EB)–CSA $_{0·5\ mol}$ at 442 nm, PANI(EB)–CSA $_{0·4\ mol}$ at 444 nm, PANI(EB)–CSA $_{0·3\ mol}$ at 451 nm is given. The doping of PANI(EB) with the CSA converts the insulating nature of PANI(EB) into conducting state (metallic nature) because the protons of CSA are added to –N= sites while the number of electron in the chain are

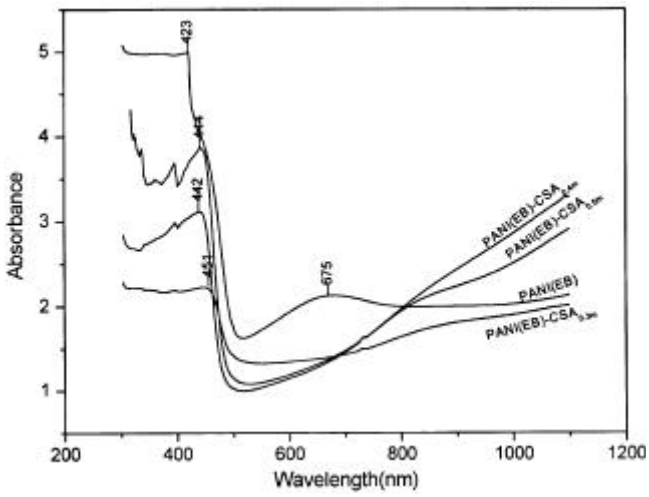

Figure 3. Absorption spectra of PANI(EB)–CSA$_X$ polymer cast films.

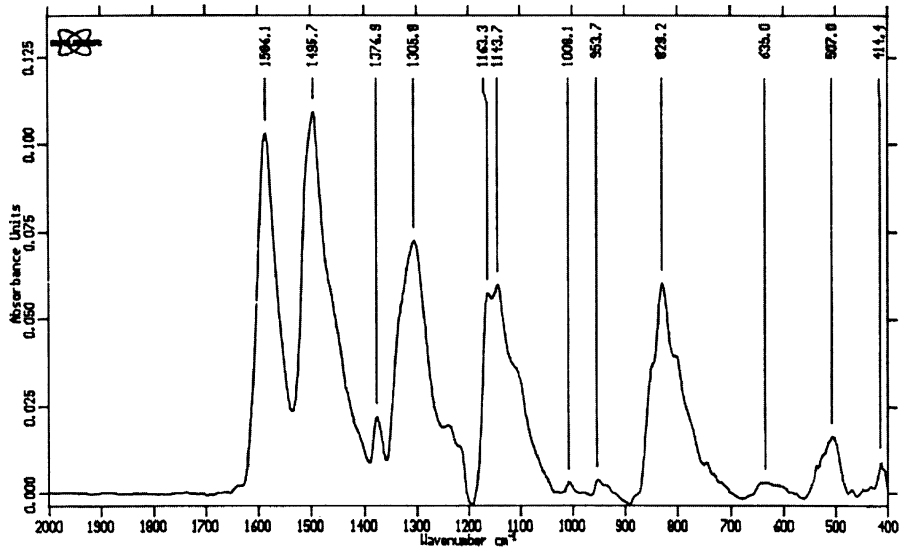

Figure 2. FTIR absorbance spectra of PANI(EB) polymer.

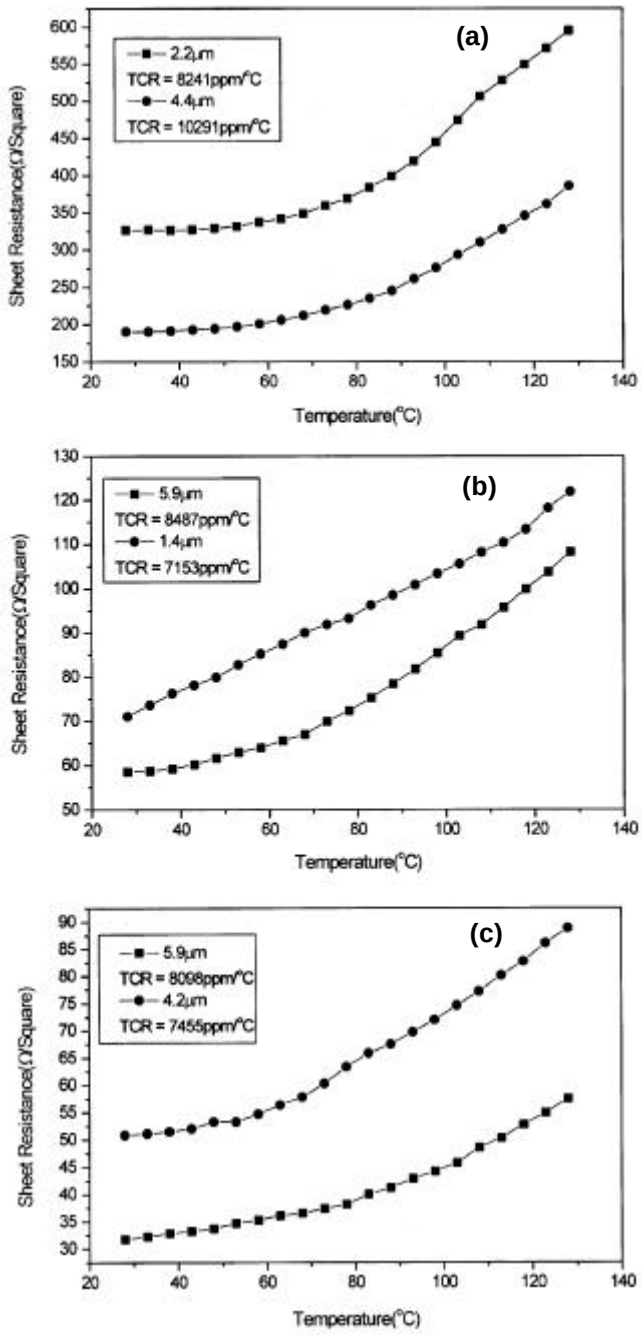

Figure 4. Sheet resistance response versus temperature plots of PANI(EB)–CSA_X polymer solution cast films on glass substrates. **a.** PANI(EB)–$CSA_{0·3}$ mol, **b.** PANI(EB)–$CSA_{0·4\ mol}$ and **c.** PANI(EB)–$CSA_{0·5\ mol}$.

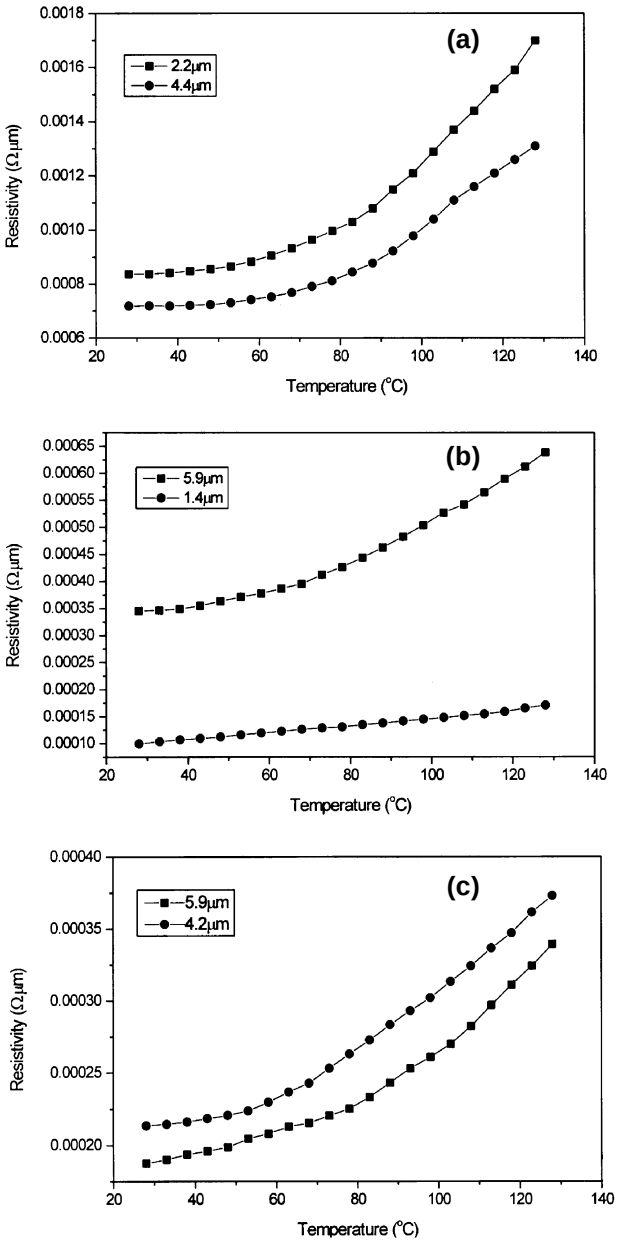

Figure 5. Temperature dependence resistivity plots of PANI (EB)–CSA_X polymer solution cast films on glass substrates. **a.** PANI(EB)–$CSA_{0·3\ mol}$, **b.** PANI(EB)–$CSA_{0·4\ mol}$ and **c.** PANI (EB)–$CSA_{0·5\ mol}$.

constant. Because of this reason all the doped polymer films absorption spectra extend to the infrared without absorption peak at 675 nm. So, the red shift occurs in all the doped cases.

3.3 *Electrical properties*

Figure 4 shows the sheet resistance response vs temperature plots of PANI(EB)–CSA_X (X = 0·5, 0·4, 0·3 mol) polymer solutions cast films on glass substrates with two different film thicknesses in each doping ratio. The temperature coefficient of resistance (a) values were obtained from the slopes of those plots in the temperature region 28–128°C. Corresponding film resistivity vs temperature plots are shown in figure 5. From these plots, we observed metal like behaviour in these polymer films. This transition from insulator to metal happens after the doping of CSA with insulating emeraldine base form of polyaniline, because protons of CSA are added to the –N= sites also. The number of electrons in the chain are

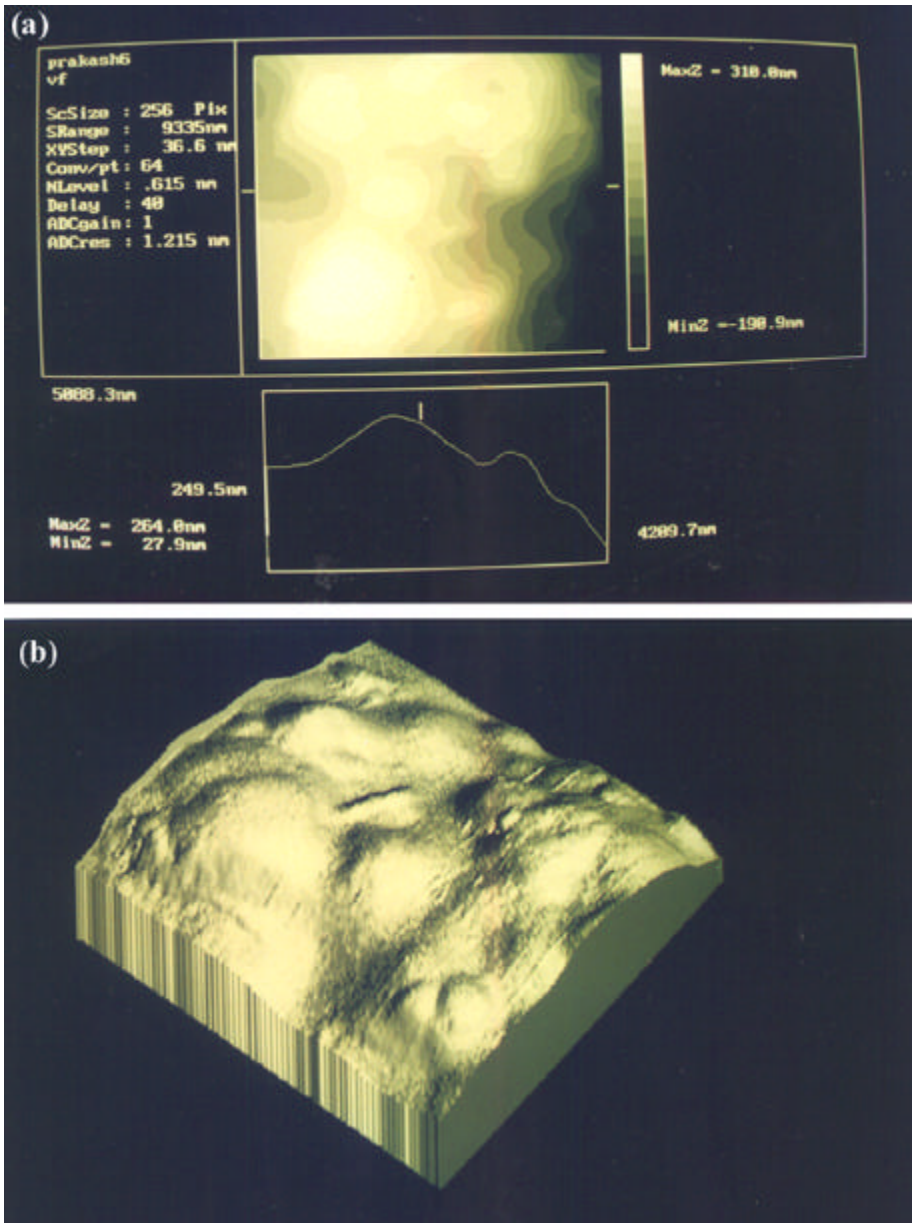

Figure 6. The AFM images of PANI(EB)–CSA$_{0\cdot3\ mol}$ polymer film (4·4 μm thick): (**a**) two-dimensional image and (**b**) three-dimensional image.

constant. The product of resistivity (r) with temperature coefficient of resistance (a) values gives figure of merit (ra) value of films, the a, r and ra values of these films are tabulated in table 1. Also, well known commonly used thermal sensitivity materials like Ni, Pt and alloy based metal films (Maissel and Glang 1970; CRC Handbook 1983) together with recently reported (Sundeen and Buchanan 2001) cermet films are tabulated in table 2. Table 2 is useful to compare PANI(EB)–CSA$_X$ polymer films thermal sensitivity with other materials. In both the tables the materials used are metal films only, but the film deposition technique and substrates used are different. Beyond this difference the high temperature coefficient of resistance (TCR) values and wide resistivity (r) values of these PANI(EB)–CSA$_{0\cdot3\ mol}$ polymer film (4·4 μm thick) seems to be the best for developing thermal sensors because of their high TCR (10,291 ppm/°C) values and resistivity range 718–1309 Ω·μm.

3.4 *AFM studies*

The surface morphological examination of PANI(EB)–CSA$_{0\cdot3\ mol}$ polymer film (4·4 μm thick) observed by AFM in two-dimensional views are shown in figures 6a and b, respectively. For this AFM scan, we scanned the film in ~ 9300 nm square area with ruggedness scale

Table 1. Thermal sensor characteristics of PANI(EB)–CSA_X polymer films.

Sl. no.	Polymer films	Thickness (μm)	TCR (ppm/°C)	r (Ω·μm)	ra (Ω·m/°C)
1.	PANI(EB)–$CSA_{0·5\ mol}$	5·9	8098	187–339	1·33–2·42
		4·2	7455	214–373	1·59–2·78
2.·	PANI(EB)–$CSA_{0·4\ mol}$	5·9	8487	346–639	2·93–5·42
		1·4	7153	99–170	0·71–1·22
3.	PANI(EB)–$CSA_{0·3\ mol}$	4·4	10291	718–1309	5·91–10·78
		2·2	8241	838–1699	8·62–17·48

Table 2. Thermal sensor characteristics of pure metals and selected Ni–ZrO_2 films (Sundeen and Buchanan 2001).

Material	Thickness (μm)	TCR (25–125°C) (ppm/°C)	r (μΩ cm)	ra (Ω cm/°C)·10^{-8}
Ni†	–	6400–6800	6·80	~ 4·2
Pt†	–	3860–3930	10·20	~ 3·9
Au†	–	3900–4000	2·22	~ 0·9
Ag†	–	3800–4100	1·55	~ 0·6
Cu†	–	4100–4300	1·57	~ 0·7
55 vol.% Ni–ZrO_2	~ 1·0	2600–4000	425–6000	170–1560
55 vol.% Ni–Y*	~ 1·0	2850–3400	1250–7300	430–2090
45 vol.% Ni–La*	~ 1·0	2515	65000	16350

†Ni, Pt, Au, Ag, Cu: literature values; *dopant oxide (10 mol.%).

height 310 nm. The three-dimensional view shows that this film is not perfectly smooth and it has a globule of 246 nm height with aggregates of tiny globules. This nature is acceptable because of the film depositing technique used is solution casting. But we may get perfectly smooth films in other polymer film deposition methods like spin casting and dip coating.

4. Conclusions

The present investigations of PANI(EB)–CSA_X polymer films produced by solution casting method have been shown to exhibit high a, relative wide resistivity, r, and therefore, a high figure of merit ra product compared to other thermal sensing materials, which have typically been utilized in heat sensing operations. In these polymer films the electrical properties and optical characterization together with AFM scans offer superior thermal sensor properties and the advantages of developing 'polymer thermal sensors' with PANI(EB)–CSA_X polymer materials.

Acknowledgements

We gratefully acknowledge the academic advice and support received from Prof. S Ramasamy, Department of Nuclear Physics, University of Madras, Chennai. We also thank the Research scholars of Thin Film Laboratory, Physics and Botany Departments, Bharathiar University, Coimbatore, for their timely help.

References

Cao Y, Lee K and Heeger A J 1995 *Synth. Metals* **69** 261

Chopra K L 1969 in *Thin film phenomena* (New York: McGraw-Hill) 2nd ed.

Chopra K L and Kaur Inderjeet 1983 in *Thin film device applications* (New York: Plenum Press) 1st ed.

CRC 1983 *Handbook of chemistry and physics*, 64th ed.

Geng Yanhou, Li Ji, Sun Zeicheng, Jing Xiabin and Wang Fosong 1998 *Synth. Metals* **96** 1

Maissel L I and Glang G 1970 in *Handbook of thin film technology* (New York: McGraw-Hill) 3rd ed.

Mott N F and Jones H 1958 in *The theory of the properties of metals and alloys* (New York: Dover)

Pouget J P, Jozefowicz M E, MacDiarmid A G and Epstein A J 1991 *Macromolecules* **24** 779

Sundeen J E and Buchanan R O 2001 *Sensors and Actuators* **A90** 118

Tang J S, Jing X B, Wang B C and Wang F S 1989 *Synth. Metals* **24** 231

Tang J S, Jing X B, Wang X H and Wang F S 1996 *Synth. Metals* **69** 93